DOI: 10.31401/WS.2024.proc.10

St. Patrick's Day 2015 Geomagnetic Storm: Sources of Perturbations

Stefan C., Dobrica V.

"Sabba S. Stefanescu" Institute of Geodynamics of the Romanian Academy,
19-21 Jean-Louis Calderon St., 020032 Bucharest, Romania; cristiana_stefan@geodin.ro

Abstract

The St. Patrick's Day 2015 geomagnetic storm, the strongest one of the solar cycle 24, was analyzed in order to highlight the possible sources accountable for the perturbations observed in recorded data during the storm. SuperMAG database was used to obtain ground data recordings in an equally distributed grid at the northern hemisphere scale that then were analyzed by means of the empirical orthogonal function method (EOF). The connection between the time series of the EOF modes and various geomagnetic indices (Dst, AE) that describe current systems in the magnetosphere and ionosphere, sources of perturbations, was achieved using the wavelet coherence analysis (WTC).

Keywords: Sun-Earth interaction; St. Patrick's Day 2015 geomagnetic storm; sources of perturbations

Introduction

The strongest geomagnetic storm of solar cycle 24 that occurred on 17 March 2015 is associated to a partial halo coronal mass ejection (CME) related to a C9.1 flare. It was first seen in LASCO/C2 images at 02:00 UT on March 15 and wasn't expected to reach Earth. The unexpected arrival was, as proposed by Kataoka et al. (2015), due a combination of (1) a fast CME followed by a high-speed stream from a nearby coronal hole and (2) a preceding slow and high-density CIR that was piled up ahead of the CME just before the arrival at the Earth enhancing its magnetic field and density. This "pileup accident" as named by Kataoka et al. (2015) generated a major magnetic storm (Kp=8) with a peak in the Dst index of -234 nT reached at 23:00 UT. Carter et al. (2016) investigated the impact of this storm in terms of geomagnetically induced currents (GICs), produced by induced geoelectric fields that are caused by magnetic field fluctuations, using magnetometer data from around the world. Dobrica et al. (2016) and Demetrescu et al. (2018) calculated the induced geoelectric field using data recorded at European geomagnetic observatories.

In order to identify the sources responsible for the perturbations observed in ground data during the development of the St. Patrick's Day 2015 geomagnetic storm we applied two widely used methods in meteorology and oceanography, namely the EOF/PCA (von Storch and Navarra, 1995; Hannachi, 2004) and the wavelet coherence (Grinsted et al., 2004). According to Bjornsson and Venegas (1997) the EOF method facilitates the determination of the spatial distribution of the variability modes (EOF) of a given field, their associated temporal variations (PC) and their importance in terms of variance. The wavelet coherence analysis (Grinsted et al., 2004) investigates relationships in time-frequency space between two time series and shows locally phase locked behavior. In geomagnetism the EOF/PCA was used by Pais et al. (2015), Domingos et al. (2019) and Stefan et al. (2019-2020) on geomagnetic field models data to show various characteristics of the geomagnetic field. Recently, Morozova and Rebbah (2023) used the PCA method to remove the Sq variation from the geomagnetic field data. The wavelet coherence (WTC) analysis was used by Giri et al. (2024) to show the phase relation between the plasma beta, Alfven Mach number, and magnetosonic Mach number with SYM-H index in case of four geomagnetic storms from solar cycles 23, 24 and 25.

Data and method

The SuperMAG database was used to acquire 1 minute data in an even spatial grid at the northern hemisphere scale. The data is available at https://supermag.jhuapl.edu/. We choose a six days interval such so the storm to be in the middle of the analyzed interval and also have information about the geomagnetic conditions prior of the storm as well on the end of the recovery phase. The EOF/PCA method was used to decompose the geomagnetic field data recorded during the 17 March 2015 geomagnetic storm into variation modes in order to highlight the possible sources of the perturbations observed in ground data. The geomagnetic indices Dst (SYM-H, ASY-H) and AE (AO, AU, AL), that describe current systems from the magnetosphere and ionosphere, sources of perturbations, were used. The data for both indices is available at http://wdc.kugi.kyoto-u.ac.jp/aeasy/index.html.

In order to show the relationship between various geomagnetic indices, which are proxies for different current systems from the magnetosphere and ionosphere, and the temporal variations associated to the EOF modes we used the wavelet coherence analysis (WTC) (Grinsted et al., 2004).

Results and discussion

The distribution, at the northern hemisphere scale, of the north geomagnetic field component (X) at the minimum of the Dst (Figure 1) shows a depression of the field of about 600 nT in the most affected area, namely the southern part of the Scandinavian Peninsula. Also, an about 400 nT decrease in the field took place in the north-west of Russia.

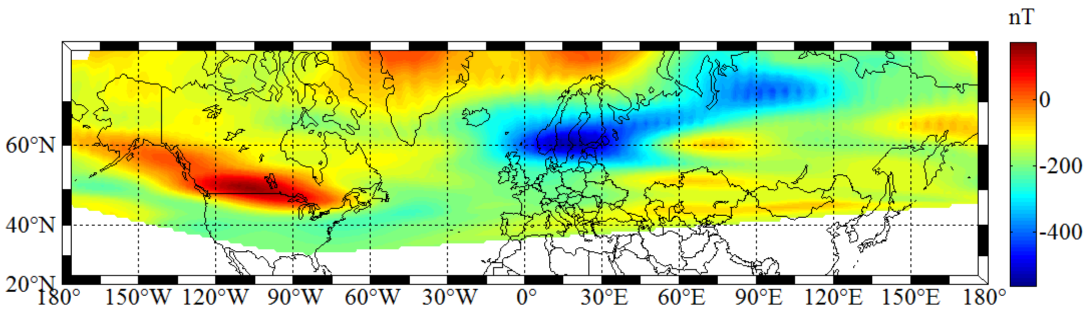

Figure 1. *Geographical distribution of the north geomagnetic field component (X) at the minimum of the Dst*

The geographical distribution of the first EOF mode (~68% variance) (Figure 2, left) reveals that the most affected areas were the Scandinavian Peninsula, the northern part of the North Atlantic, Greenland, the north-east and central Canada, North Dakota and Montana from the US. Lower intensity perturbations affected Alaska, north-west and west of the Canadian territory and Russia. The graphical representation of the time series of the first mode (PC1) along with the SYM-H index (Figure 2, upper right) reveals that there is a very good correlation (correlation coefficient -0.97) between the two of them. Also, the wavelet coherence analysis (Figure 2, bottom right) shows that the two times series are phase locked even before the beginning of the storm, marked on the figure with the purple rectangle. Based on this information we can state that almost 68% of the observed perturbations in ground data is due to the ring current intensification that takes place during the storm.

The second EOF mode (Figure 3, left) is responsible for 13% of the disturbed signal in recorded data and can be associated with the intensification of the auroral electrojet represented by the AU index. The wavelet coherence analysis (Figure 3, bottom right) reveals that before the commencement of the storm, in the time interval 30 minutes – 2 hours, there is a link between AU index and the time series of the second EOF mode (PC2). In the time interval of the duration of the storm (purple rectangle on the figure) there is a clear coherence between the analyzed time series.

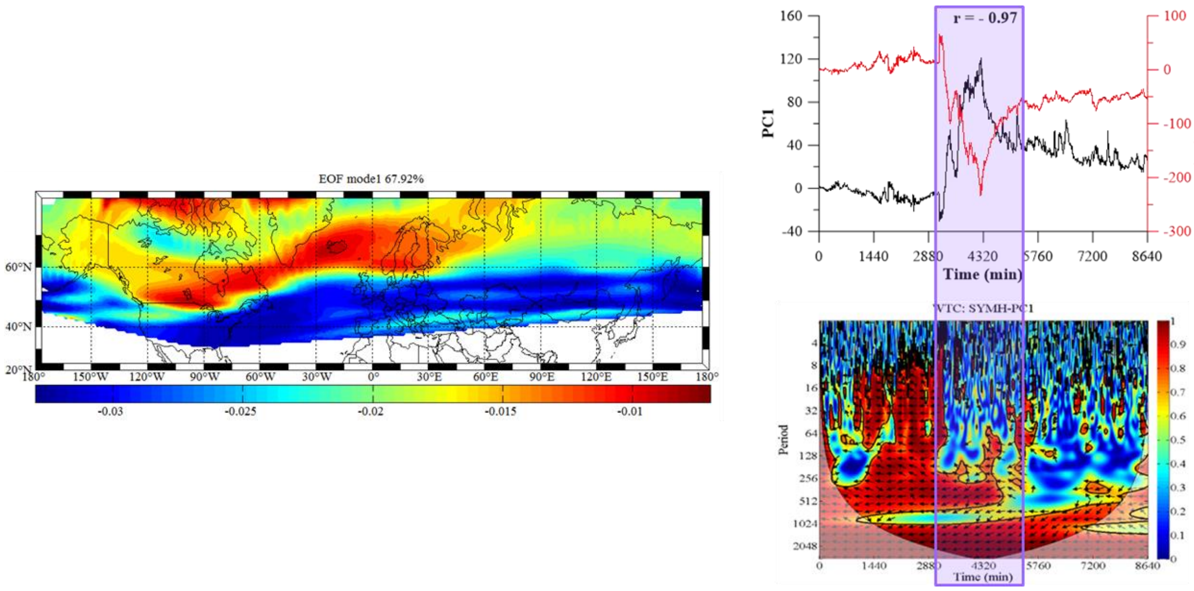

***Figure 2**. Geographical distribution of the first EOF mode (left) and the associated PC1 series (black line) along with the geomagnetic index SYM-H (red line), respectively the coherence between PC1-SYM-H (bottom). The period of the storm is marked by the purple rectangle*

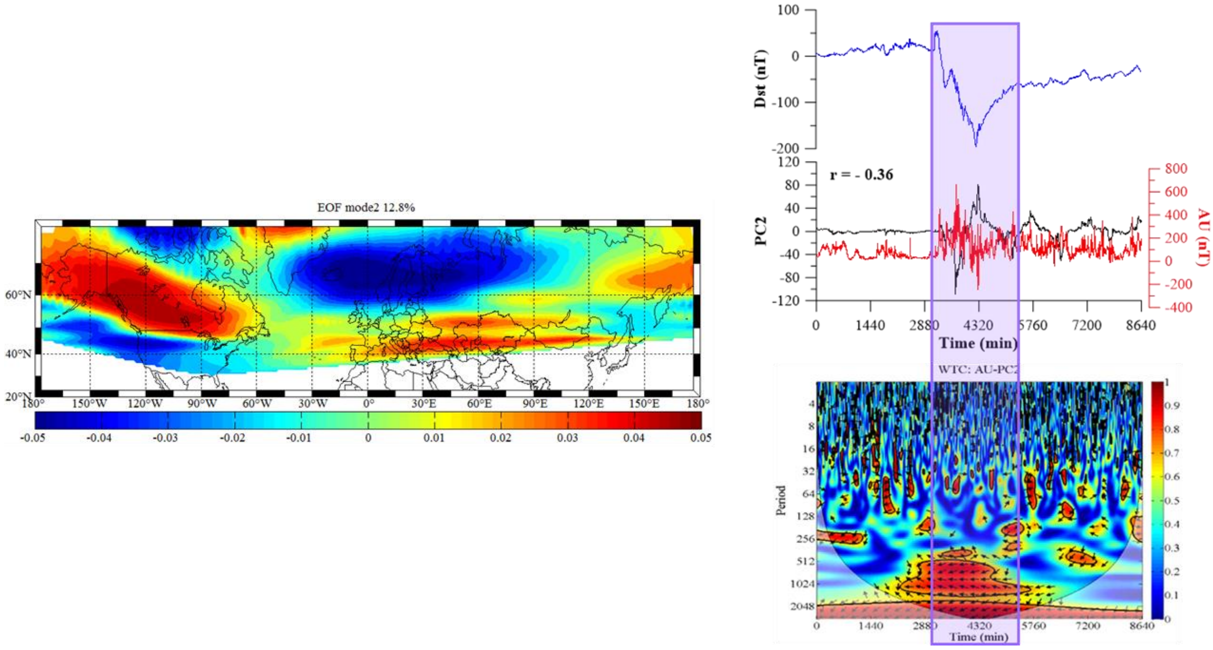

***Figure 3.** Geographical distribution of the second EOF mode (left) and the associated PC2 series (black line) along with the geomagnetic indices Dst (blue line) and AU (red line), respectively the coherence between PC2-AU (bottom). The period of the storm is marked by the purple rectangle*

In Figure 4 (left) is represented the third mode that accounts for about 9% of the overall perturbation; it can be associated with the AO. The WTC shows that there is mostly an in-phase relationship (arrows pointing right) between the time series of mode 3 (PC3) and the AO index (Figure 4, bottom right).

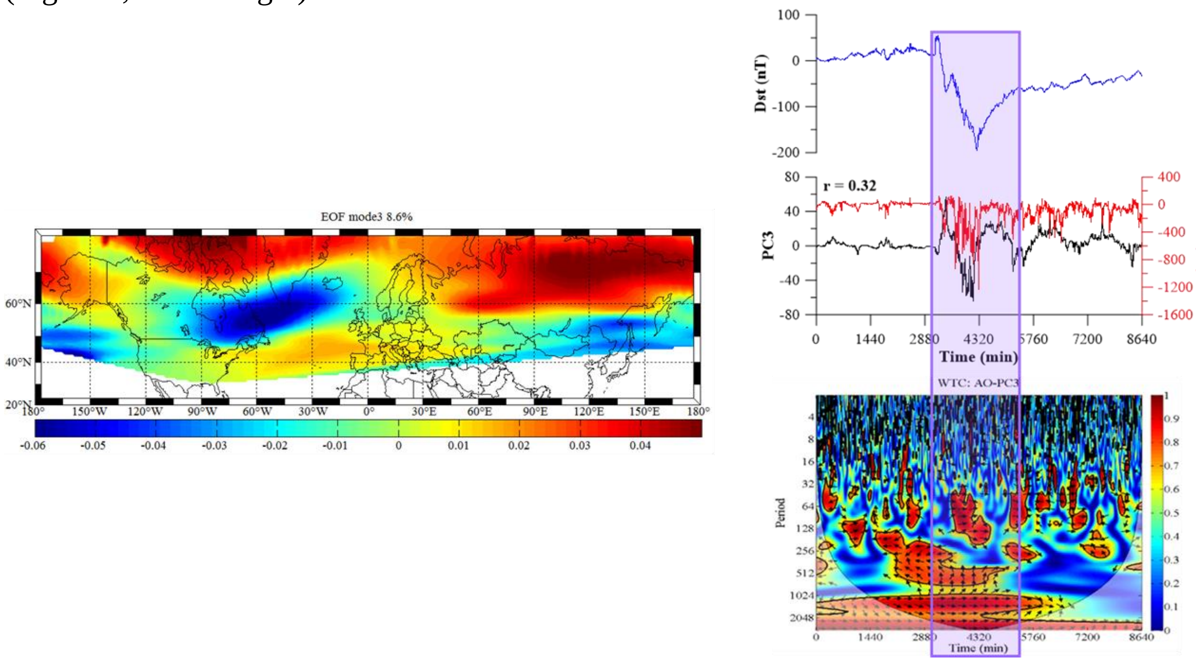

Figure 4. *Geographical distribution of the third EOF mode (left) and the associated PC3 series (black line) along with the geomagnetic indices Dst (blue line) and AO (red line), respectively the coherence between PC3-AO (bottom). The period of the storm is marked by the purple rectangle*

Conclusions

Applying two widely used methods in meteorology and oceanography and relatively new introduced in geomagnetism, namely EOF/PCA and wavelet coherence we were able to identify the sources accountable for the perturbations observed in geomagnetic data during the St. Patrick's Day 2015 storm. We obtained that the main source for this perturbations is given by the intensification of the ring current that takes place during the storm.

Acknowledgements

The paper is a contribution to the Project 3/2023 of the Institute of Geodynamics of the Romanian Academy.

Crosswavelet and wavelet coherence software were provided by A. Grinsted.

References

Bjornsson, H., Venegas, S.A. (1997), A manual for EOF and SVD analyses of climate data, Tech. Rep. No. 97-1, Department of Atmospheric and Oceanic Sciences and Centre for Climate and Global Change Research, McGill University.

Carter, B. A., Yizengaw, E., Pradipta, R., Weygand, J. M., Piersanti, Pulkkinen, M., A., Moldwin, M. B., Norman, R., Zhang, K. (2016), Geomagnetically induced currents around the world during the 17 March 2015 storm, J. Geophys. Res. Space Physics, 121, 10,496–10,507, doi:10.1002/2016JA023344.

Demetrescu, C., Dobrica V., Greculeasa, R., Stefan, C. (2018). The induced surface electric response in Europe to 2015 St. Patrick's Day geomagnetic storm, J. Atmos. and Sol. Terr. Phys., 180,106-115.

Dobrica, V., Demetrescu, C., Stefan, C., Greculeasa, R. (2016). Geomagnetically Induced Currents, a space weather hazard. Case study – Europe under intense geomagnetic storms of the solar cycle 23. Sun Geosph. 11, 111–117.

Domingos, J., Pais, M.A., Jault, D., Mandea, M. (2019). Temporal resolution of internal magnetic field modes from satellite data, Earth Planets Space 71, 2. https://doi.org/10.1186/s40623-018-0983-5.

Giri, A., Adhikari, B., Baral, R., Idosa Uga, C., Calabia, A. (2024). Wavelet Coherence Analysis of Plasma Beta, Alfven Mach Number, and Magnetosonic Mach Number during Different Geomagnetic Storms, The Scientific World Journal, 2024, 1335844, 11 pages. https://doi.org/10.1155/2024/1335844.

Grinsted, A., Moore, J.C., Jevrejeva, S. (2004). Application of the cross wavelet transform and wavelet coherence to geophysical time series, Nonlin. Processes Geophys. 11, 561–566, doi:10.5194/npg-11-561-2004.

Hannachi, A. (2004). A Primer for EOF Analysis of Climate Data, Department of Meteorology, University of Reading, 33pp.

Kataoka, R., Shiita, D., Kilpua, E., Keika, K. (2015). Pileup accident hypothesis of magnetic storm on 17 March 2015, Geophys. Res. Lett. 42(13): 5155–5161. https://doi.org/10.1002/2015GL064816.

Morozova, A., Rebbah, R. (2023). Principal component analysis as a tool to extract Sq variation from the geomagnetic field observations: Conditions of applicability, MethodsX, 10, 101999. https://doi.org/10.1016/j.mex.2023.101999

Pais, M.A., Morozova, A.L., Schaeffer, N. (2015). Variability modes in core flows inverted from geomagnetic field models. Geophys J Int 200:402–420. doi:10.1093/gji/ggu403.

Stefan, C., Dobrica, V., Demetrescu, C. (2019-2020). Geomagnetic field characteristics revealed by empirical orthogonal functions, Rev. Roum. GÉOPHYSIQUE, 63–64, p. 63– 67.

Von Storch, H., Navarra, A. (1995). Analysis of Climate Variability: Applications of Statistical Techniques, Springer, 334pp, doi:10.1007/978-3-662-03167-4.